Marine Pollution Bulletin 75 (2013) 114–125

Contents lists available at ScienceDirect

Marine Pollution Bulletin

journal homepage: www.elsevier.com/locate/marpolbul

# Benthic foraminiferal assemblages and trace metals reveal the environment outside the Pearl River Estuary

Tao Li [a,b,*], Rong Xiang [c], Tuanjie Li [b]

[a] Guangzhou Marine Geological Survey, Guangzhou 510760, People's Republic of China
[b] South China Sea Marine Engineering Surveying Center, State Oceanic Administration, Guangzhou 510300, People's Republic of China
[c] South China Sea Institute of Oceanology, Chinese Academy of Science, Guangzhou 510301, People's Republic of China

ARTICLE INFO

*Keywords:*
Benthic foraminifera
Population characteristics
Trace metal
Statistical analysis
Pearl River Estuary

ABSTRACT

We investigated the distribution patterns of the benthic foraminiferal assemblages outside the Pearl River Estuary in relation to trace metals, organic carbon and sedimentary particle fractions. The study area is unpolluted to moderately polluted by Cr, Cu, Pb and Zn and is completely polluted by Ni. The highest levels are found in the western coastal zone. Spatial distributions of the measured elements are strongly related to the behavior of the sedimentary clay fraction. The analyses of species abundance and community diversity as well as subsequent canonical correspondence analysis were used to reveal the relationship between foraminifera data and environmental parameters. Four sampling site groups established by factor analysis were distributed from the coastal area to the inner shelf. Their distribution patterns have a strong correlation with Cu, Pb and Ba. This research shows that benthic foraminifera can be used as bioindicators of trace metal pollutants outside the Pearl River Estuary.



## 1. Introduction

Sediment contamination by trace metals in estuaries and adjacent coastal areas has become an issue of increasing environmental concern. Such pollution is mainly caused by nonpoint source runoff and human activities, including industrial, domestic, agricultural, mining, fishing, shipping and other activities that produce waste containing metal residues. The massive amount of pollution has adverse effects on the marine ecosystem, is toxic to living resources and is hazardous to human health.

Benthic foraminifera are a powerful tool for the analysis and assessment of recent and ancient marine environments owing to their small size, abundance and well preserved shells (Murray, 2000). The distribution, abundance, and diversity of benthic forams depend on water depth, sediment texture and the physicochemical characteristics of sediments (Murray, 2006). Variation in any attribute can lead to a modification of the behavior and metabolism of individual species as well as the whole community. Previous syntheses of the foraminiferal community in polluted ecosystems have demonstrated that benthic foraminifera provide one of the most sensitive markers available for detecting coastal sediment contamination (Frontalini and Coccioni, 2011). These studies are mainly based on the attribution of different foraminiferal features to particular polluted sites by comparison with foraminifera detected in clean environments. Trace metals, which pollute the aquatic environment, are ultimately deposited on coastal marine sediments and impact foraminifera by modifying their community structure (Pati and Patra, 2012). In the majority of studies, a trace metal-induced environmental stress on benthic foraminiferal communities is measured via a correlation between biotic and abiotic data (Alve et al., 2009; Frontalini et al., 2009; Frontalini and Coccioni, 2008). The Pearson correlation coefficient, which is sensitive only to a linear relationship between two variables, is the most common tool for measuring the degree of correlation. However, the significance of such correlations is questionable if synergistic effects exist (Alve et al., 2009). Subsequently, multivariate approaches are used to distinguish the effect of the available pollutants from mixed influencing factors and allow for a quantitative evaluation (Eichler et al., 2012; Frontalini and Coccioni, 2008; Martins et al., 2010, 2013; Romano et al., 2008; Teodoro et al., 2010). Most studies have shown that foraminiferal assemblages in polluted areas have extremely low species numbers and diversity compared with those in non-polluted areas (Bergamin et al., 2009, 2005; Debenay and Fernandez, 2009; Elberling et al., 2003; Ferraroa et al., 2006; Samir, 2000; Schafer, 1973; Yanko et al., 1998). Nevertheless, an increased pollution level was reportedly the cause of an increased abundance of certain species, which is typical when species become tolerant to special trace metals (Alve and Olsgard, 1999; Armynot du Châtelet

* Corresponding author. Address: Room 412, Jidi Building, No. 188 Guanghai Road, HuangPu District, Guangzhou, People's Republic of China. Tel.: +86 020 82030197.
*E-mail address:* lukelitao80@163.com (T. Li).

0025-326X/$ - see front matter © 2013 Elsevier Ltd. All rights reserved.
http://dx.doi.org/10.1016/j.marpolbul.2013.07.055

et al., 2004, 2011; Bergamin et al., 2009, 2003; Debenay et al., 2001; Foster et al., 2012; Frontalini and Coccioni, 2008; Le Cadre and Debenay, 2006; Romano et al., 2009, 2008).

This work aims to (1) identify the distribution patterns of benthic foraminiferal assemblages outside the Pearl River Estuary, (2) reveal the relationship between the spatial distribution of trace metals and the dispersion of sedimentary material, and (3) examine the variance of foraminiferal assemblages in relation to available environmental variables.

## 2. Study area

The Pearl River Estuary is located on the south coast of China and connects to the northern continental shelf of the South China Sea. Three principal tributaries, namely, West River, North River and East River, flow into the Pearl River (see Fig. 1a). The Pearl River is the largest river system of the South China Sea, and the annual water flow rate of this river is approximately 11,100 $m^3/s$ (Wong et al., 1995).

The study area is located outside of the Pearl River Estuary and its surrounding coastal area. It extends from the offshore area of Shangchuan Island to Honghai Bay, covering an approximate area of $2 \times 10^4$ $km^2$, and the water depths range from 2 m to 100 m (Fig. 1b). Bathymetrically, this area can be divided into two parts: (1) the coastal marine area, which is shallower than 20 m, and (2) the inner shelf, which is deeper than 20 m.

The entire study area is mainly influenced by three different hydrodynamic systems: the Pearl River discharge, oceanic waters from the South China Sea and coastal waters from the South China Coastal Current (Yin et al., 2000). In winter, the northeast monsoon prevails, and the South China Coastal Current controls the coastal currents. In summer, the southwest monsoon dominates, and the interaction between the estuarine plume and the oceanic waters plays a leading role.

## 3. Materials and methods

### 3.1. Sediment sampling

Surface sediment samples were collected with a grab using a boat at 246 sites during the summer of 2005. The boat's sonar was used to measure the water depth, and a differential global positioning system (DGPS) was used to locate the sites (Appendix A). The surface sediment samples were collected at the selected locations. Only the top ~5 cm of sediment was retained for analysis. The bathymetry of the study area is shown in Fig. 1b along with the location of the sites selected.

### 3.2. Foraminiferal analysis

All samples were dried at 50 °C and weighed. Subsequently, the samples were gently washed through a 63-μm sieve with tap water to remove clay and silt. The residual fractions were re-dried at 50 °C and weighed to determine the mass of the mud fraction. Quantitative analyses on benthic foraminifera were performed on the fraction larger than 150 μm, and total foraminiferal assemblages were counted. The minimum number of specimens used in statistical analysis was approximately 100 for each sample. The counts were standardized as percentages.

Several parameters linked to the assemblages were calculated, including the species abundance (defined as the total number of individuals per 50 g of dried sediment), the species richness (number of species per sample), the Shannon–Weaver index $H(S)$ (describes the species diversity in a community) (Shannon, 1948), and the Fisher $\alpha$ index (measures the mean species diversity) (Fisher et al., 1943). The multivariate statistic software PRIMER v5 (Plymouth Routines In Multivariate Ecological Research) was used in the calculation of the $H(S)$ and the Fisher $\alpha$ index (Clarke and Gorley, 2001).

### 3.3. Trace metal and organic carbon analysis

The second set of samples was dried, reduced to a fine powder and used to determine trace metal contents in sediments. Wuhan Mineral Resources Supervision and Inspection Center (Ministry of Land and Resources, P.R.C.) analyzed a fraction of each sample (0.4–4 g) to determine the levels of 20 elements using an X-ray fluorescence spectrometer (PW2440 (MagiX Pro), Panalytical company, Holland). A series of geochemical standards were used as controls. In this work, only the concentrations of Ba, Co, Cr, Cu, Ni, Pb, Sr, V, Zn and Zr were evaluated. The detection limits for trace metals were Ba: 7.2 mg $kg^{-1}$, Co: 0.7 mg $kg^{-1}$, Cr: 2 mg $kg^{-1}$, Cu: 1 mg $kg^{-1}$, Ni: 0.7 mg $kg^{-1}$, Pb: 2 mg $kg^{-1}$, Sr: 0.8 mg $kg^{-1}$, V: 5 mg $kg^{-1}$, Zn: 2 mg $kg^{-1}$, and Zr: 1 mg $kg^{-1}$.

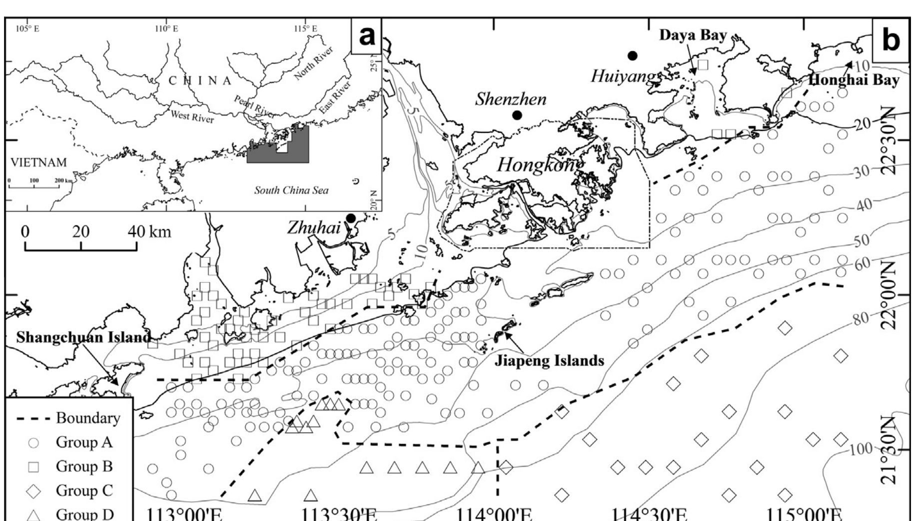


Fig. 1. Maps showing the study area (a) and the sampling locations (b). Site coordinates are included in Appendix 1. Samples are grouped based on the results of factor analysis.

The percentage of organic carbon was determined by titration with ferrous ammonium sulfate after dissolution in potassium dichromate sulfuric acid solution.

### 3.4. Grain size and sediment transport analysis

Samples used for grain size analysis were treated with $H_2O_2$ solution, sieved and dried at 40 °C. Grain size analysis was performed to determine the percentage of silt and clay (<63 μm) using a Mastersizer 2000 laser particle size analyzer (Malvern Instruments Ltd., UK), and the sand fraction (63 μm to 2 μm) was separated using a micro-sieve. The grain size classification system proposed by Shepard (1954) was followed. Grain size parameters (mean size, sorting, skewness and kurtosis) were calculated using the GRADISTAT program (v. 8.0) (http://www.kpal.co.uk/gradistat.html) (Blott and Pye, 2001). The results are presented in Appendix C.

Sediment transport analysis (STA) was performed using a point-to-point 2D model developed by Gao and Collins (Gao, 1996). Trend vectors, which represent net transport paths, were determined via a grid of sampling sites comparing three granulometric parameters (mean size, sorting and skewness) between neighboring samples (Gao and Collins, 1992, 1994a,b). In this study, neighboring sampling sites were identified on the basis of a characteristic distance ($D_{cr}$) defined by the maximum sampling interval (equal to 10.2 km) according to the suggestion of (Gao and Collins, 1991).

### 3.5. Statistical analysis

All statistical analyses were performed on the relative proportion of each species. Only species exceeding 5% of the assemblage in at least one sample were considered to reduce the background noise. R-mode factor analysis was performed with the SPSS (Statistical Product and Service Solutions) software package using the percentage of each species to facilitate the establishment of foraminiferal assemblages. Pearson correlations were used to reveal the correlations between abiotic and biotic parameters. Canonical correspondence analysis (CCA), a multivariate technique devoted to niche separation along environmental variables, was executed using the CANOCO (v. 4.5) software package and was used to summarize the benthic foraminiferal community data and to relate these data to a set of measured environment parameters.

## 4. Results

### 4.1. Grain size distribution patterns

Sediment grain size and composition were heterogeneous throughout the sampling area (Fig. 2a). The mean percentages of sand, silt and clay were 22.6%, 60.4% and 17%, respectively; sediment mean size varied from 1 to 8.49$\Phi$ (mean 5.79$\Phi$), and sediment sorting and skewness varied from 0.6 to 3.72 (mean 1.92) and −1.54 to 4.58 (mean 0.3) (Appendix C). Sediments from the coastal marine area were dominated by clayey silt (the eastern area) and silt (the western area). In the inner shelf, a high proportion of sand and silty sand occurred in the eastern area, whereas silt and sandy silt were common in the western area.

### 4.2. Organic carbon and trace metal contents

Organic carbon content varied from 0.1% to 2%, with a mean content of 0.9%. The maximum levels (>1%) were found in the coastal marine area (Fig. 2b). Concentrations of trace metals varied widely throughout the study area (Appendix C, Fig. 2). The minimum, mean and maximum values of each trace metal were summarized in Table 1.

Maps of the concentrations of Ba, Co, Cr, Cu, Ni, Pb, Sr, V, Zn and Zr were included in Fig. 2, and these elements generally showed different patterns of distribution compared with the other chemical elements. Barium (Fig. 2c) had distribution patterns similar to those of Zr (Fig. 2l). The concentration ranges of Ba and Zr were 300–400 mg kg$^{-1}$ and 200–400 mg kg$^{-1}$, respectively, at most of the sampling sites, and the concentration levels of these metals are below the median in the western area of the inner shelf. Cobalt (Fig. 2d), Cr (Fig. 2e), Ni (Fig. 2g), V (Fig. 2j) and Zn (Fig. 2k) shared the same distribution pattern. Metal concentrations in the sediments (in mg kg$^{-1}$) ranged from 10 to 15 for Co, 60 to 90 for Cr, 20 to 40 for Ni, 80 to 120 for V, and 60 to 120 for Zn. The variation in the concentrations of these metals was not large in the eastern section of the study area; however, the concentrations varied more in the western section of the study area, with the maximum concentration observed in shallow water and the minimum concentration observed in deep water. Copper (Fig. 2f) had a distribution pattern similar to Pb (Fig. 2h). The concentrations of Cu and Pb decreased with an increase in water depth in the coastal area, whereas the concentrations were lower and varied slightly in the inner shelf, with Cu enrichment (exceeding the median content) noted at several sites southwest of the Jiapeng Inlands (see Figs. 2f and 1b). Strontium (Fig. 2i) showed a trend of increasing concentration from the coastal marine area to the inner shelf, and its concentration was highest (500 mg kg$^{-1}$) at sites near the 100 m isobath.

The trace metal concentrations can be compared to the adverse biological effect values, ERL (effect range low) and ERM (effect range median), in marine and estuarine sediments proposed by the U.S. National Oceanic and Atmospheric Administration (Ligero et al., 2002; Long et al., 1995). The concentrations of Cr, Cu, Pb, and Zn were below ERL at most of the sampling sites, representing an unpolluted to moderately polluted setting. The sites that were most polluted (exceeding ERL) by these elements were located in the western coastal zone. Additionally, a few sites polluted by Cu were located in the eastern coastal zone. Nickel was verified as a widespread pollutant in the study area, whose concentrations were generally higher than ERL but lower than ERM.

### 4.3. Benthic foraminiferal distribution

The main 52 benthic foraminifera species identified in this study belonged to 30 genera (Appendix B). In general, the foraminiferal assemblages in the study area were largely dominated by *Ammonia tepida*, *Hanzawaia nipponica*, *Ammonia ketienziensis*, *Elphidium advenum*, *Ammonia compressiuscula*, *Florilus japonicus*, *Heterolepa dutemplei*, and *Gavelinopsis prageri*. Foraminiferal assemblages were composed of mixtures of hyaline walls, agglutinated walls and porcelaneous walls, which make up 87.9%, 7.1%, and 5% of the total, respectively. Hyaline foraminifera occurred at all sites analyzed; however, agglutinated species were enriched at sites near the river mouth. Porcelaneous types were commonly observed in areas partially covered with coarse-grained sand, and this type accounted for low to very low percentages of assemblages elsewhere. The ratio between agglutinated and calcareous foraminiferal tests (A/C) was extremely low at the study area, with a mean value of 0.1. Species richness (Fig. 3a), which varied from 6 to 52, was generally higher in the eastern area than in the western area. Species abundance (Fig. 3b) ranged from hundreds to a few thousand individuals per 50 g of dry sediment in the coastal area and ranged from 10,000 to 100,000 individuals per 50 g of dry sediment in the inner shelf area. Diversity indices varied from 0.3 to 3.5 for $H(S)$ and from 0.8 to 12 for the Fisher $\alpha$ index. There was a linear relationship between Fisher $\alpha$ and $H(S)$, although the correlation was weak ($r^2 = 0.418$). These two

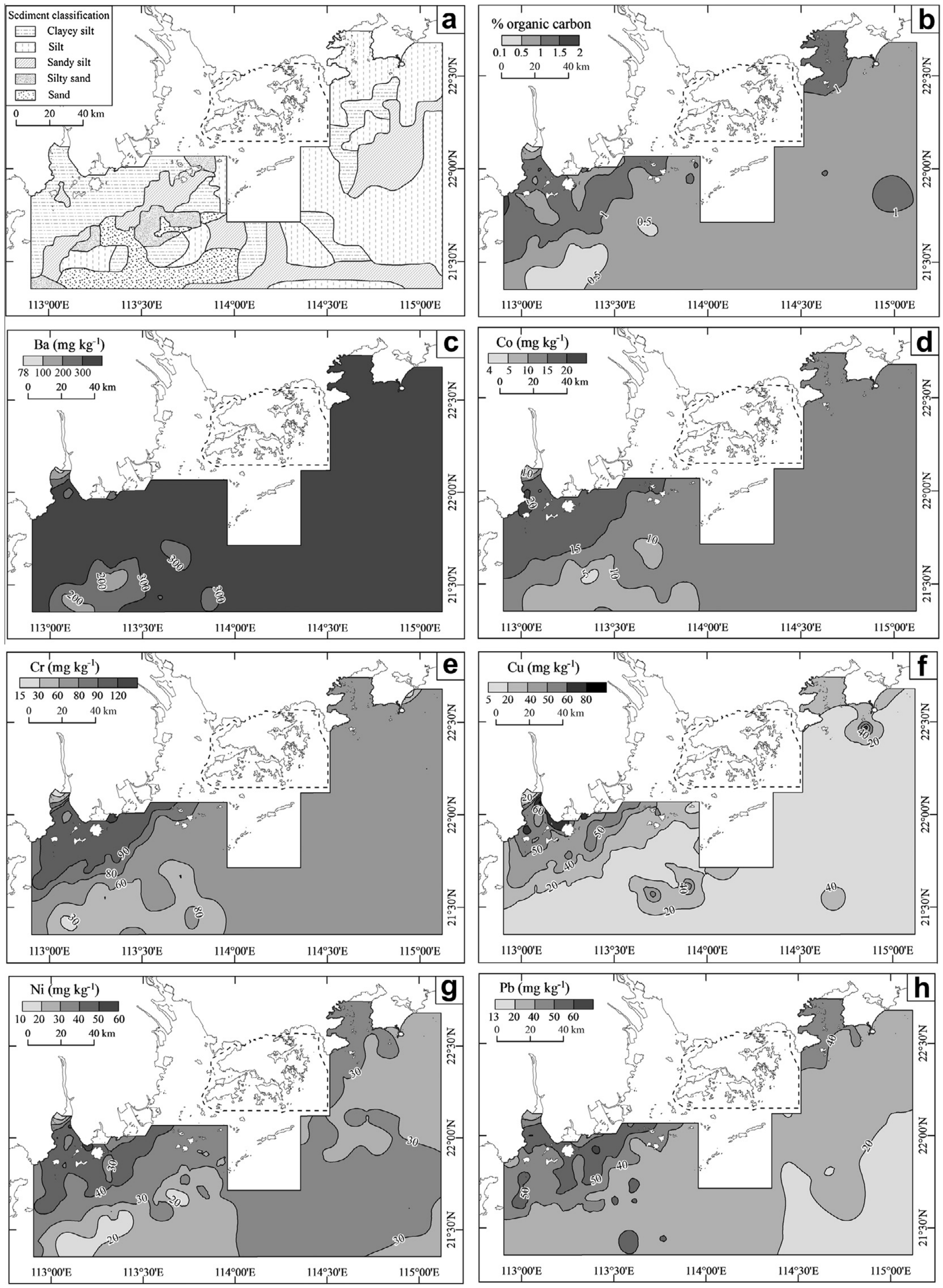


**Fig. 2.** Spatial distributions of sediments (a), percentages of organic carbon (b), and concentrations of the following trace metals: Ba (c), Co (d), Cr (e), Cu (f), Ni (g), Pb (h), Sr (i), V (j), Zn (k), and Zr (l).

indices were lower in the western coastal zone and generally increased with increasing distance from the west coast (Fig. 3 c and d).

Ammoniatepida was the major species in the coastal marine area. Percentages of *Ammonia tepida* (Fig. 4a) decreased with increasing water depth, and this species was absent in deeper areas (exceeding 30–40 m depth). These individuals were the most abundant species in the coastal area, exceeding 30% of the total, and they also dominated (10–30% of the total) the foraminiferal assemblages at sites near the 20 m isobath. *Hanzawaia nipponica Ammonia ketienziensis* and *Elphidium advenum* were the dominant species in the inner shelf. *Hanzawaia nipponica* (Fig. 4b) was the most abundant species in the eastern area at a depth of 20–40 m and in the western area at a depth of 30–50 m, constituting 25–35% of the total. *Ammonia ketienziensis* (Fig. 4c) was enriched in the eastern area at depths of 20–30 m and in the western area at depths of 20–60 m, ranging from 10% to 30% of the total. *Elphidium advenum* (Fig. 4d) was abundant in the eastern area at a water depth of 20–40 m and in the western area at a water depth of 10–30 m. Percentages of*Ammonia compressiuscula* (Fig. 4e) were relatively high (10–25% of the total) in the eastern region of the

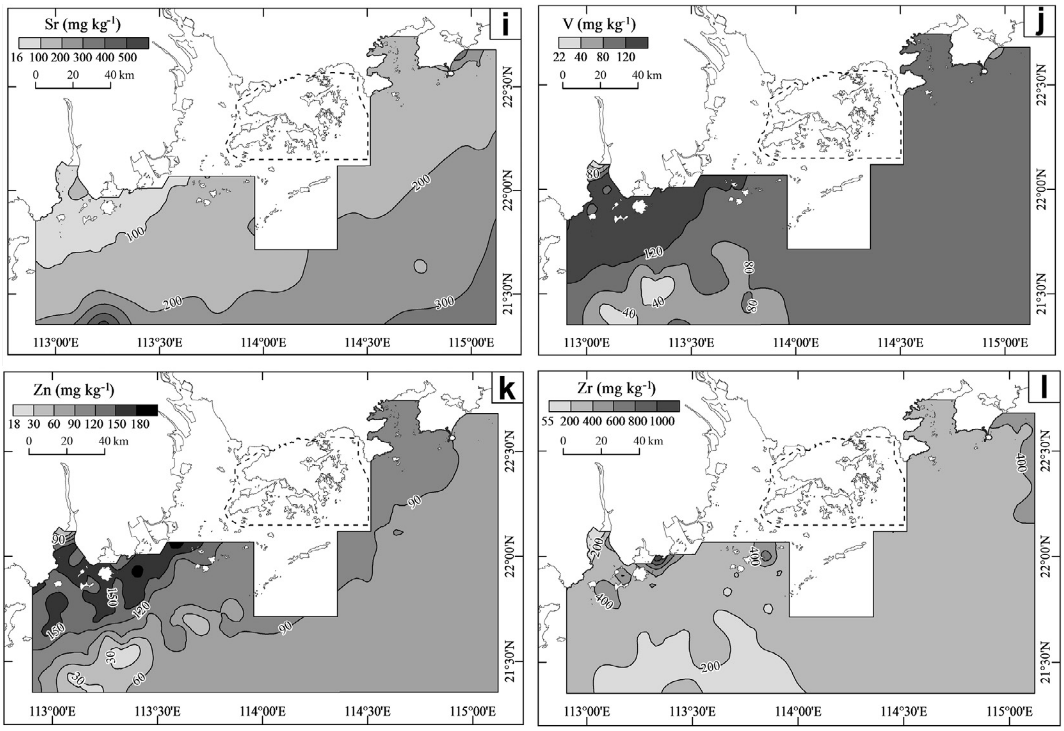


**Fig. 2** (*continued*)

**Table 1**
Basic statistics of trace metals along with ERL (effect range low) and ERM (effect range median) values. nd, not determined.

| | Ba | Co | Cr | Cu | Ni | Pb | Sr | V | Zn | Zr |
|---|---|---|---|---|---|---|---|---|---|---|
| Mean | 334.45 | 13.38 | 73.87 | 25.13 | 32.47 | 36.98 | 150.90 | 102.91 | 105.10 | 294.76 |
| Min | 63.5 | 4.1 | 10.7 | 2.1 | 9.4 | 13.5 | 16.5 | 15.0 | 20.5 | 56.8 |
| Max | 372.1 | 21.5 | 137.8 | 90.5 | 56.2 | 62.9 | 561.3 | 167.9 | 192.0 | 5345.3 |
| Stand. dev. | 38.45 | 3.37 | 16.77 | 16.35 | 7.35 | 11.18 | 62.52 | 27.76 | 34.83 | 342.69 |
| ERL | nd | nd | 81 | 20.9 | 20.9 | 46.7 | nd | nd | 150 | nd |
| ERM | nd | nd | 270 | 51.6 | 51.6 | 218 | nd | nd | 410 | nd |

study area at water depths between 10 m and 30 m. *Florilus japonicus* (Fig. 4f) was distributed widely throughout the study area, although its numbers were relatively low (i.e., it accounts for a few hundredths of the total). *Heterolepa dutemplei* (Fig. 4g) dominated (15–30% of the total) the foraminiferal assemblages in the western area of the inner shelf. This species was absent in the coastal area. *Gavelinopsis prageri* (Fig. 4h) was the most abundant species (10–20% of the total) in the eastern region of the inner shelf at water depths between 40 m and 80 m.

### 4.4. Factor analysis

In a previous investigation (Li et al., 2011), four varimax rotated factors were retained in the R-mode factor analysis. Together, they explained 86.5% of the total variance of the benthic foraminifera data set. Factor 1, 2, 3 and 4 loadings established four sampling site groups, labeled A through D.

Group A included sampling sites with high scores for factor 1 and occupied the inner shelf area in the western region shallower than 40 m and area in the eastern region shallower than 60 m (see Figs. 5a and 1b). The area occupied by this group was covered by a variety of sediments, the most abundant of which were clayey silt, silt and sandy silt. This group was characterized by a low $H(S)$ (mean, 2.45) and Fisher $\alpha$ index (mean, 4.6) and comparatively high species richness (mean, 30) and abundance (mean, 25,000). The dominant species in this group were *Hanzawaia nipponica*,*Ammonia ketienziensis*, *Elphidium advenum*, *Ammonia compressiuscula*, *Florilus japonicus*, *Elphidium asiaticum*,*Florilus scaphus*, *Elphidium magellanicum*, and *Fursenkoina schreibersiana*.

Group B consisted of sampling sites with high scores for factor 2 and was distributed in the coastal marine area (see Figs. 5b and 1b), which was mostly covered with clayey silt (the western region) and silt (the eastern region). This group was characterized by a significantly low $H(S)$ (mean, 2.15), Fisher $\alpha$ index (mean, 3.37), species richness (mean, 18) and abundance (mean, 5000). The characteristic species in this group included *Ammonia tepida*, *Elphidium nakanokawaense Cavarotalia annectens*, *Arenoparella asiatica Ammoscalaria* sp., *Ammobaculites agglutinans*, *Cribrononion* sp., and *Haplophragmoides canariensis*.

Group C was characterized by sampling sites with high scores for factor 3 and encompassed sites located in the eastern region of the inner shelf at water depths of 60–100 m (see Figs. 5c and 1b) with sediments including silt and sandy silt. This group was characterized by a high $H(S)$ (mean, 3.03), Fisher $\alpha$ index (mean, 5.17), species richness (mean, 38) and abundance (mean, 36,000). The most abundant species in this group were *Gavelinopsis prageri*, *Cassidulina carinata*, *Cassidulina laevigata*, *Astrononion* spp., *Ammonia pauciloculata*, *Bolivina robusta*, *Hanzawaia nipponica*, *Bulimina maginata*, *Cibicides praecinctus*, and *Pulsiphonina elegana*.

Group D encompassed sampling sites with high scores for factor 4 and was distributed in the western region of the inner shelf at water depths of 35–60 m (see Figs. 5d and 1b) with sediments

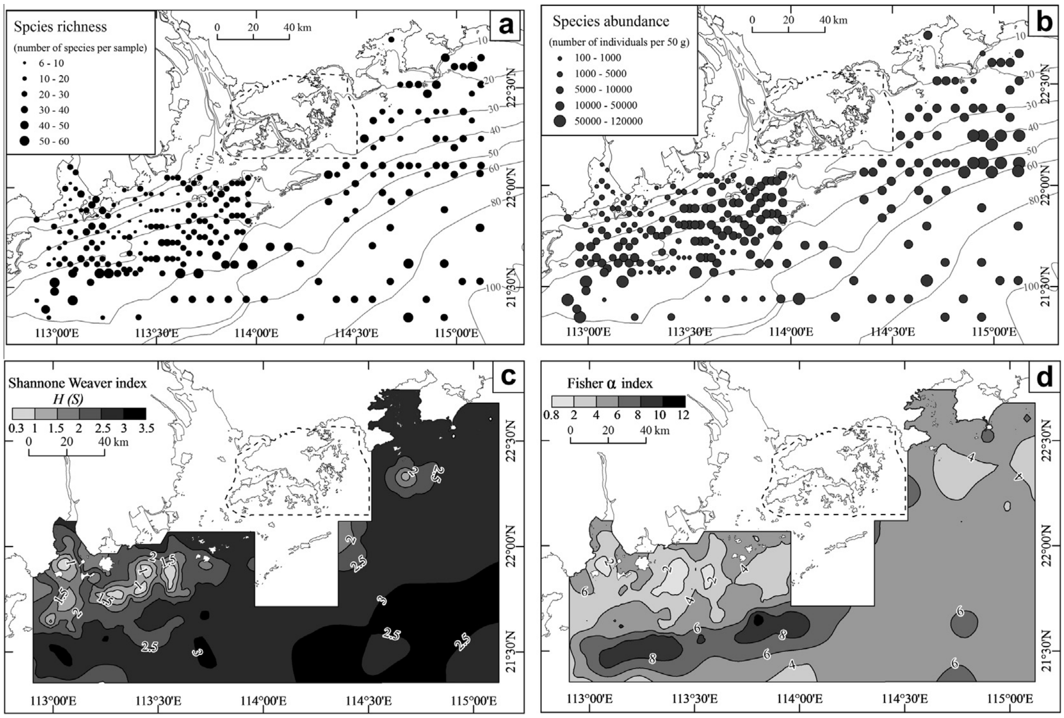


**Fig. 3.** Spatial distributions of the species diversity indices of benthic foraminiferal assemblages: species richness (number of species per sample) (a), species abundance (number of species) (b), Shannon–Weaver index ($H(S)$) (c), and Fisher $\alpha$ index (d).

containing a high proportion of coarse-grained sand. This group was characterized by a relatively high $H(S)$ (mean, 2.63) and Fisher $\alpha$ index (mean, 5.07) as well as a low species richness (mean, 23) and abundance (mean, 3600). The most common species in this group were *Heterolepa dutemplei*, *Textularia foliacea*, *Textularia paragglutinans*, *Quinqueloculina akneriana*, *Amphistegina radiata*, *Bigenerina nodosaria*, *Triloculina tricarinata*, *Triloculina trigonula*, *Quinqueloculina larmarckiana*, and *Quinqueloculina pseudoreticulata*.

### 4.5. Correlation analysis

The similarity between biotic and abiotic parameters was investigated using correlation analysis (Table 2). The correlation matrix revealed a marked, negative influence of trace metal (Cu, Pb, Co, Cr, Ni, V and Zn) on the $H(S)$, Fisher $\alpha$ index, species richness and abundance, and certain foraminifera species (i.e., *Bolivina robusta*, *Cassidulina laevigata*, *Gavelinopsis prageri*, *Hanzawaia nipponica*, *Heterolepa dutemplei*, *Textularia foliacea*, and *Textularia paragglutinans*) while a positive influence was observed for *Ammonia tepida Cavarotalia annectens*. The opposite correlations were observed between Sr and the diversity indices and most of these species. Barium has positive correlations with some species such as *Ammonia compressiuscula*, *Ammonia ketienziensis*, *Bolivina robusta*, *Elphidium advenum*, *Elphidium asiaticum*, and *Gavelinopsis prageri*, and negative with species such as *Heterolepa dutemplei*, *Quinqueloculina akneriana*, and *Textularia paragglutinans*.

### 4.6. Canonical correspondence analysis

The CCA outputs were summarized in Table 3. Monte Carlo permutation tests revealed that all the measured parameters, except for silt, qualified for interpretation of the total variance in the foraminifera data set ($p < 0.05$). Partial analysis showed that the total explained variability was 56.3%. The interpreted variance percentages of the parameters were presented in Fig. 6, which illustrated that Ba, Sr, Pb, Zn, Zr, organic carbon, sand, Cr, V, Ni, Cu, Co, and clay separately explained 10.4%, 8.6%, 7.5%, 6.4%, 5.1%, 4.3%, 3.7%, 3.2%, 3.2%, 2.3%, 2.1%, 1.7%, and 1.1%, respectively, of the variance in the foraminiferal assemblage component.

The CCA results were also shown in sample-environment and species-environment bi-plots (Fig. 7). The positioning of species or sample projected on the bi-plots and environmental variables were represented by arrows. The $A1$ axis had an eigenvalue of 0.499, and the $A2$ axis had an eigenvalue of 0.194. The species-environment correlations obtained from CCA for axes $A1$ and $A2$ were 0.893 and 0.808, respectively.

The angles between the arrows representing the environmental variables and the CCA axes can be used to approximate the correlations between these variables and the CCA axes. From the angles, we could predict that the $A1$ axis (the main explainable variation in the foraminiferal community composition) was slightly positively correlated with Ni, Zn, Cr, Co, and V and negatively correlated with Sr; additionally, it had a larger positive correlation with Cu and Pb. The $A2$ axis was highly negatively correlated with Ba, and it had a weak positive correlation with sand.

The four sampling site groups, established on the basis of factor loadings, were also distinguished in the CCA bi-plots. The position and separation of the sites along the $A1$ axis indicated that sites with positive scores on the $A1$ axis correlated positively with Cu and Pb. Group B projected on the positive side of the $A1$ axis, whereas groups C and D and most of group A projected on the negative side of the $A1$ axis. Hence, group B was separated on the $A1$ axis. Groups C and D and most of group B projected on the positive side of the $A2$ axis, whereas the majority of group A projected on the negative side of the $A2$ axis. We inferred that group A could be separated on the $A2$ axis. Species showed similar relationships under the same environmental conditions.

## 5. Discussion

### 5.1. Distribution patterns of trace elements and sediment transport

Estuarine sediments are recognized as an important sink for trace elements and other contaminants (Ip et al., 2004). Trace

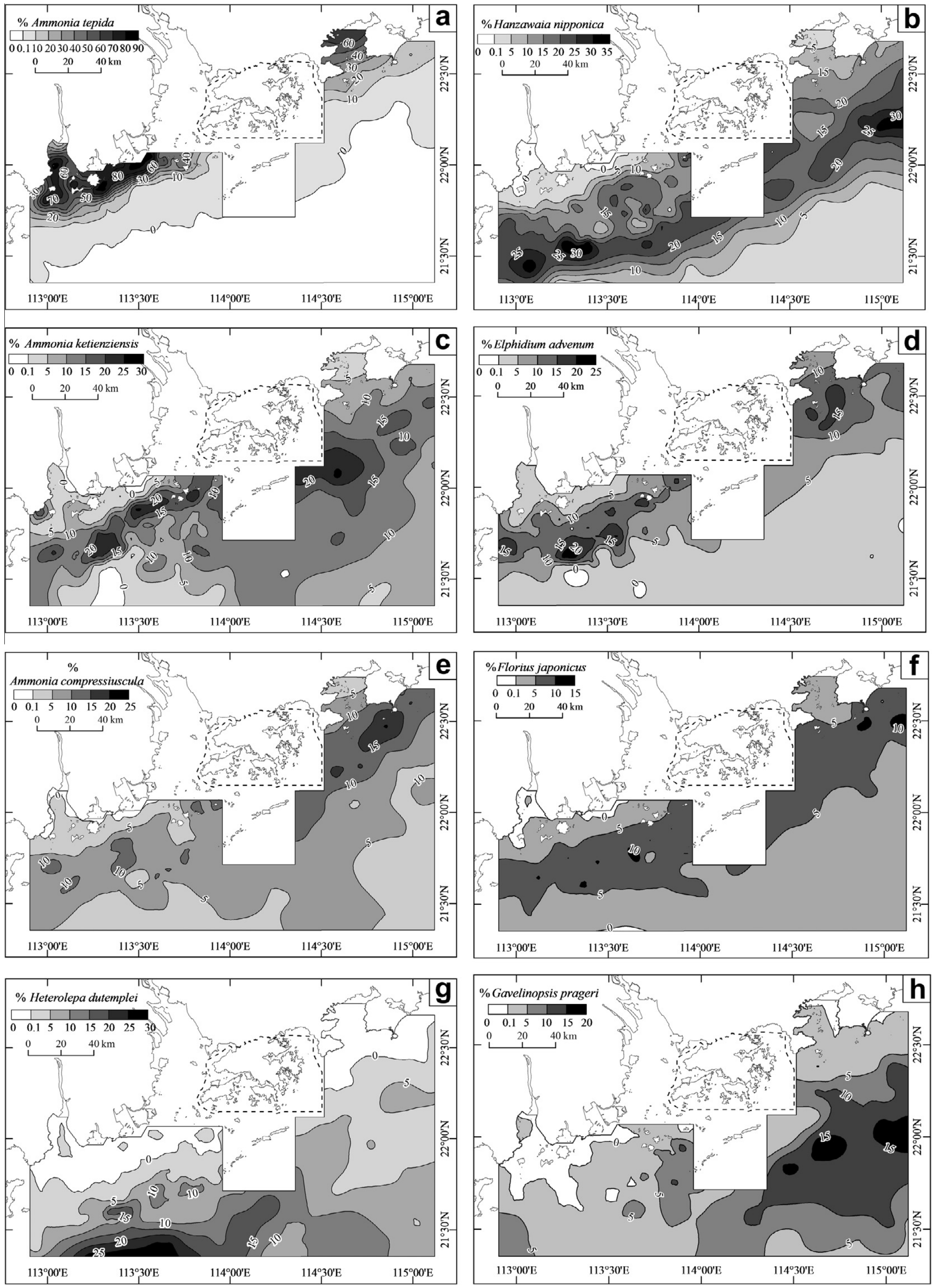


**Fig. 4.** Spatial distributions of the dominant components (constituting more than 5% of the total on average) of benthic foraminiferal assemblages: *Ammonia beccarii* (a), *Hanzawaia nipponica* (b), *Ammonia ketienziensis* (c), *Elphidium advenum* (d), *Ammonia compressiuscula* (e), and *Florilus japonicus* (f).

metal pollutants, once released, enter hydrological circulation and are finally deposited in marine sediments. Trace metals in water preferentially adsorb to cohesive sediments, which are composed primarily of clay and fine silt components. Hence, the transfer of trace element pollutants through the aquatic environment is strongly related to the behavior of the fine particle fraction of sediment deposited from suspension (Milligan and Loring, 1997; Ongley et al., 1992). In this study, most of the measured elements (i.e., Ba, Co, Cr, Cu, Ni, Pb, V and Zn) have a significant positive correlation with the sedimentary clay fraction (Table 2).

The dynamics of sediment entrainment, transport and deposition are controlled by sediment particles. Sediment transport analysis (STA) based on grain size provides important clues to the sediment provenance, transport history and depositional conditions (Blott and Pye, 2001). The net transport and dispersion of sedimentary material, as determined by the application of Gao and

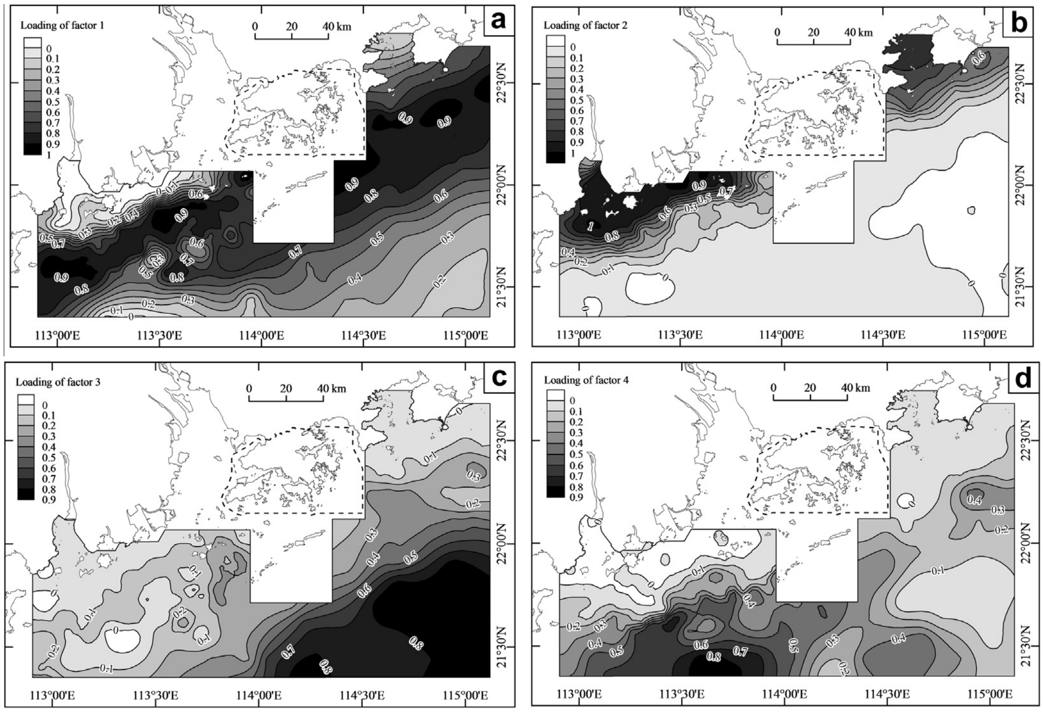


**Fig. 5.** Spatial distributions of factor loading of R-mode factor analysis based on benthic foraminiferal assemblages.

**Table 2**
Pearson correlation matrix between foraminiferal assemblages and abiotic parameters at the stations. Values ($p < 0.05$, two-tailed test) are in bold.

| | Organic carbon | Ba | Co | Cr | Cu | Ni | Pb | Sr | V | Zn | Zr |
|---|---|---|---|---|---|---|---|---|---|---|---|
| Sand | **−0.38** | **−0.44** | **−0.38** | **−0.34** | −0.20 | **−0.36** | −0.03 | 0.17 | **−0.39** | **−0.36** | 0.13 |
| Silt | **0.31** | **0.44** | **0.27** | **0.26** | 0.08 | **0.26** | −0.10 | −0.06 | **0.28** | **0.24** | −0.12 |
| Clay | **0.37** | **0.25** | **0.48** | **0.39** | **0.41** | **0.46** | **0.34** | **−0.37** | **0.49** | **0.49** | −0.10 |
| Richness | **−0.34** | −0.02 | **−0.45** | **−0.38** | **−0.38** | **−0.42** | **−0.52** | **0.38** | **−0.46** | **−0.48** | 0.07 |
| Abundance | −0.11 | **0.26** | **−0.26** | −0.17 | **−0.43** | **−0.25** | **−0.56** | **0.43** | **−0.23** | **−0.32** | 0.04 |
| *H*(*S*) | **−0.33** | −0.13 | **−0.35** | **−0.33** | **−0.25** | **−0.33** | **−0.33** | 0.18 | **−0.37** | **−0.37** | −0.02 |
| Fisher α index | **−0.3** | −0.02 | **−0.46** | **−0.37** | **−0.4** | **−0.4** | **−0.46** | **0.38** | **−0.46** | **−0.45** | 0.05 |
| *Ammonia tepida* | **0.40** | −0.01 | **0.69** | **0.66** | **0.72** | **0.62** | **0.64** | **−0.47** | **0.65** | **0.72** | 0.07 |
| *Ammonia compressiuscula* | −0.08 | **0.22** | **−0.21** | **−0.26** | **−0.30** | **−0.25** | −0.14 | −0.03 | **−0.20** | **−0.22** | 0.03 |
| *Ammonia ketienziensis* | 0.08 | 0.39 | 0.01 | −0.02 | −0.21 | −0.03 | −0.16 | −0.02 | 0.03 | −0.04 | −0.02 |
| *Ammonia pauciloculata* | 0.02 | 0.18 | −0.05 | −0.08 | −0.16 | −0.07 | −0.10 | −0.01 | −0.05 | −0.04 | −0.05 |
| *Bolivina robusta* | −0.07 | **0.29** | **−0.20** | −0.17 | **−0.32** | −0.17 | **−0.41** | **0.23** | −0.17 | **−0.22** | −0.08 |
| *Cassidulina laevigata* | −0.09 | 0.09 | **−0.26** | −0.11 | **−0.34** | −0.16 | **−0.61** | **0.60** | **−0.22** | **−0.29** | −0.04 |
| *Cavarotalia annectens* | **0.22** | −0.03 | **0.25** | 0.19 | **0.23** | **0.20** | **0.21** | −0.18 | **0.25** | 0.18 | 0.02 |
| *Elphidium advenum* | 0.19 | **0.22** | 0.16 | 0.09 | 0.04 | 0.09 | **0.24** | **−0.27** | 0.15 | 0.13 | 0.09 |
| *Elphidium asiaticum* | 0.10 | **0.25** | 0.04 | 0.04 | −0.05 | 0.03 | −0.05 | −0.07 | 0.02 | 0.02 | 0.07 |
| *Florilus japonicus* | −0.13 | 0.12 | **−0.23** | **−0.31** | **−0.28** | **−0.27** | −0.03 | −0.15 | **−0.22** | **−0.23** | 0.01 |
| *Gavelinopsis prageri* | **−0.20** | **0.20** | **−0.36** | **−0.26** | **−0.45** | **−0.30** | **−0.64** | **0.47** | **−0.34** | **−0.40** | −0.04 |
| *Hanzawaia nipponica* | **−0.31** | 0.00 | **−0.41** | **−0.45** | **−0.44** | **−0.44** | **−0.29** | 0.05 | **−0.41** | **−0.44** | −0.04 |
| *Heterolepa dutemplei* | **−0.42** | **−0.28** | **−0.57** | **−0.51** | **−0.44** | **−0.46** | **−0.39** | **0.55** | **−0.55** | **−0.56** | −0.15 |
| *Quinqueloculina akneriana* | −0.14 | **−0.24** | **−0.21** | −0.18 | −0.10 | −0.15 | 0.05 | 0.06 | −0.17 | −0.18 | −0.08 |
| *Textularia foliacea* | **−0.33** | −0.14 | **−0.51** | **-0.50** | **−0.43** | **−0.46** | **−0.30** | 0.19 | **−0.49** | **−0.50** | −0.08 |
| *Textularia paragglutinans* | **−0.34** | **−0.31** | **−0.40** | **−0.41** | **−0.28** | **−0.39** | **−0.20** | **0.33** | **−0.40** | **−0.37** | −0.11 |

**Table 3**
Summary of CCA results from benthic foraminiferal assemblages.

| Axes | 1 | 2 | 3 | 4 | Total inertia |
|---|---|---|---|---|---|
| Eigenvalues | 0.499 | 0.194 | 0.176 | 0.081 | 2.983 |
| Species-environment correlations | 0.893 | 0.808 | 0.808 | 0.604 | |
| Cumulative percentage variance of species data | | | | | |
| | 16.7 | 23.2 | 29.1 | 31.8 | |
| Of species-environment relation | 44.2 | 61.3 | 76.9 | 84.1 | |
| Sum of all eigenvalues | | | | | 2.983 |
| Sum of all canonical eigenvalues | | | | | 1.129 |

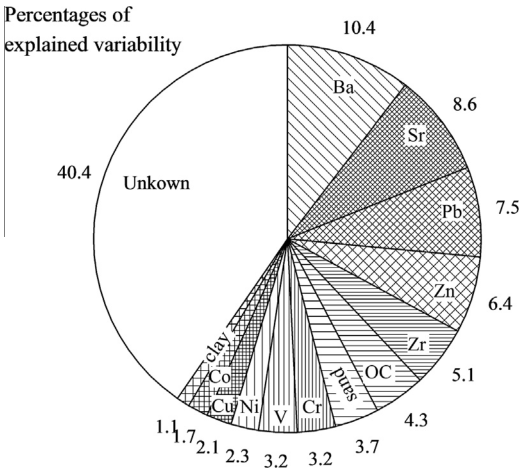


**Fig. 6.** Partitioning of variance of foraminifera species composition as explained by environmental factors.

Collins' procedure to the study area, are presented in Fig. 8. In shallow areas, the sedimentary material can be transferred by the longshore current to later be driven following a transport path perpendicular to the coast (Sánchez and Carriquiry, 2011). The transport observed in the western coastal area, which has a clear path toward the coast (Fig. 8), may indicate the transfer of materials resulting from the convergence of the South China Coastal Current (Yin et al., 2000). The coastal current flows southwestward and passes the estuary mouth, forcing the Pearl River plume to the western side of the estuary (Wong et al., 2003). The main sources of trace metal pollutants in the Pearl River estuarine area include industrial waste water, domestic sewage, marine traffic and inflow from upstream mining sites (Chen and Zhou, 1992; Li et al., 2000). Trace metals are mainly supplied by fresh water outflow via the Pearl River; consequently, relatively higher concentrations of trace metals (Co, Cr, Cu, Ni, Pb and Zn) are present in the surrounding area of the western coast (Fig. 2). The hydrodynamic effects of tidal processes, such as residual currents, may be the cause of materials exchange and transport in the eastern coastal area. The sediment is transported out of Honghai Bay with a southward component, whereas in Daya Bay, the sediment is transported into the bay in a northward direction (Fig. 8), representing a potential sink for sediment. Copper, Ni, Pb and Zn concentrations in this area are relatively high (Fig. 2). Earlier studies have revealed a rapid expansion of aquacultural, industrial and agricultural activities since the 1980s and the subsequent pollution of this area by trace

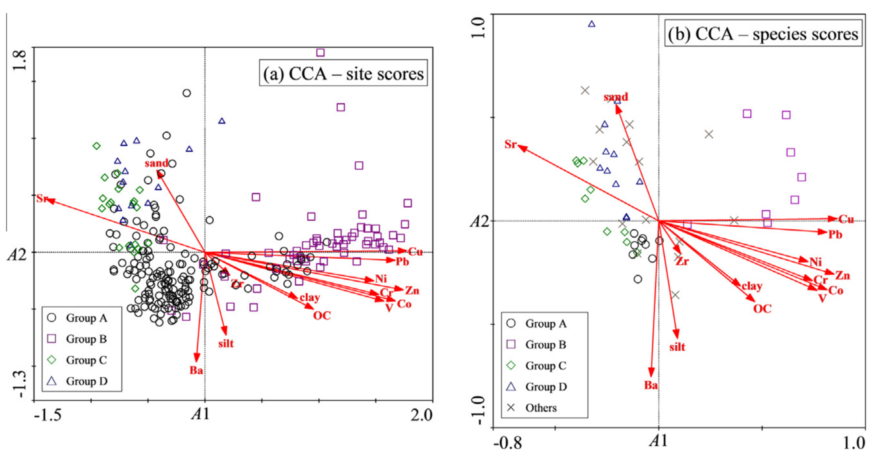


**Fig. 7.** The results of canonical correspondence analysis are shown as bi-plots of samples plotted against the measured environmental variables (a) and species plotted against the measured environmental variables (b).

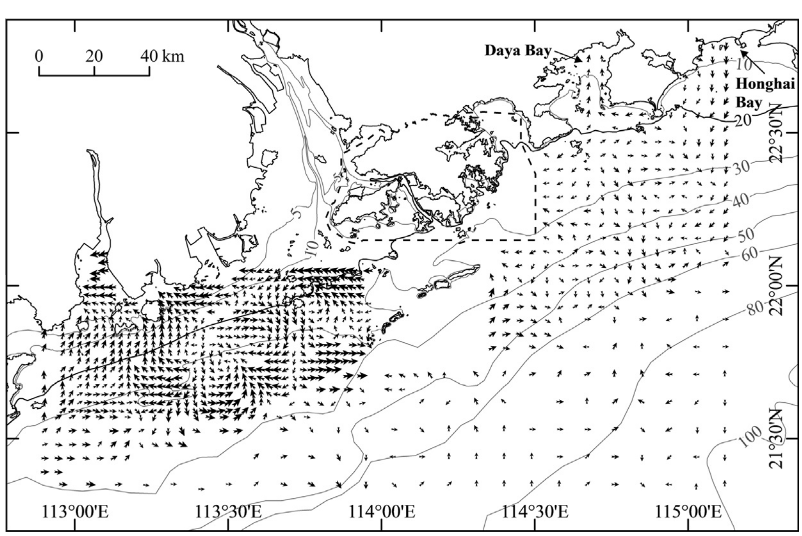


**Fig. 8.** Trend vector field defined with the method of Gao (1996). The vectors describe the net transport paths of the sedimentary material.

elements such as As, Cu, Pb and Zn (Du et al., 2008; Li, 2003; Qiu et al., 2005; Yu et al., 2010; Zheng et al., 1992). Comparatively, concentrations of trace metals (Co, Cr, Cu, Ni, Pb and Zn) in the western coastal area are significantly higher than those in the eastern coastal area, possibly because only a minority of sediment materials can be transported from the Pearl River to the eastern coastal area. The dispersal pattern of sediments in off-sea areas is affected by interactions between the estuarine plume and oceanic waters (Su, 2004). Here, the velocity of fresh water is decreased, and seawater largely dilutes the amount of pollutants contained in the sediments. In the western region of the inner shelf, where coarse-grained sand and the lowest levels of trace metals (Co, Cr, Ni, V, Zn and Zr) are encountered, the transport vectors have a general E–NE orientation (Fig. 8), indicating sediment transport toward the eastern depression. In the eastern region of the inner shelf, the sediment transport vectors show various orientations and directions, and the concentrations of trace metals (i.e., Ba, Co, Cr, Cu, Pb, V, Zn and Zr) are commonly low and vary slightly (Fig. 2).

The following four sets of trace elements can be established based on their distribution patterns: (1) Ba and Zr; (2) Co, Cr, Ni, V and Zn; (3) Cu and Pb; and (4) Sr. Based on the abovementioned dynamics of trace element entrainment, transport and deposition, the second and third sets are assumed to be composed of trace elements derived from human impacts, and anthropogenic inputs lead to the enrichment of these elements in the sediments. Additionally, the distributions of some metals partially derived from human impacts might be linked with their chemical forms and bioactivities. The chemical partitioning of trace metals in the Pearl River Estuary and the Daya Bay indicates that Cr, Ni, and Zn occur dominantly in the residual fraction, Pb is mostly found in the nonresidual fractions, and a high percentage of Cu binding to nonresidual fractions is observed in the Pearl River Estuary (Yu et al., 2010).

### 5.2. Benthic foraminiferal response to trace metal and organic matter contamination

Previous studies addressing the impact of pollutants on foraminiferal assemblages have utilized living and dead assemblages. The living foraminiferal assemblage (stained with Rose Bengal) reveals temporal changes in the absolute and relative abundance of species in relation to the sampling period (Szarek et al., 2006). Apart from seasonal variations, the total (live plus dead) foraminiferal assemblages can provide information about biological changes over a longer period (Alve et al., 2009) and have been shown to be good indicators of trace metal pollution in the past (Alve and Nagy, 1986; Armynot du Châtelet et al., 2004; Bergamin et al., 2009; Carnahan et al., 2008; Debenay et al., 2001).

Foraminiferal diversity indices have been considered indicators of trace metal pollution, and lower $H(S)$, Fisher $\alpha$ index and species abundance are usually found in polluted areas (Bergin et al., 2006). Trace metals can penetrate the foraminiferal cell with food and become toxic to benthic species (Yanko et al., 1998). Accordingly, a decreasing trend in diversity can be interpreted as a response to trace metal pollution (Bergamin et al., 2005; Debenay and Fernandez, 2009; Elberling et al., 2003; Samir, 2000; Schafer, 1973). In this study, the lowest foraminiferal diversity indices are found in the western coastal area, which is the most highly polluted by Cr, Cu, Pb and Zn. The values of these indices increase as the distance away fromthe west coast increases. The relationship between diversity and trace elements can be measured by the correlation coefficient. Diversity parameters such as $H(S)$, the Fisher $\alpha$ index and species abundance correlate negatively with Co, Cr, Cu, Ni, Pb, V and Zn (Table 2). In other estuaries, foraminiferal diversity also has a negative correlation with special trace metals (Armynot du Châtelet et al., 2004; Carnahan et al., 2008; Debenay et al., 2001).

Despite the availability of community data, the presence or absence of individual species can provide more valuable ecological information (Debenay et al., 2000). Previous researchers have demonstrated that increasing trace element content can lead to increases in the relative abundance of certain benthic species (Frontalini and Coccioni, 2008), which can be regarded as a possible indication of pollution. The currently known pollution-tolerant and opportunistic species occurring in harbors or estuarine environments polluted with trace metals include *Ammonia tepida A. parkinsoniana*, *Bolivinellina pseudopunctata*, *Bolivina variabilis*, *Cornuspira involvens*, *Cribroelphidium oceanensis*, *Elphidium advena E. excavatum E. magellanicum*, *Haynesina germanica Miliolinella subrotunda*, *Quinqueloculina bicostata*, *Q.lata*, an *Stainforthia fusiformis* (Alve and Olsgard, 1999; Armynot du Châtelet et al., 2004; Armynot du Châtelet et al., 2011; Bergamin et al., 2009, 2003; Debenay et al., 2001; Foster et al., 2012; Frontalini and Coccioni, 2008; Le Cadre and Debenay, 2006; Romano et al., 2009, 2008). In this study, *Ammonia tepida*, occasionally reported as *Ammonia beccarii*, is the only bioindicator of trace metal pollutants such as Cr, Cu, Ni, Pb and Zn. Correlation indices (Table 2) reveal that *Ammonia tepida* has a strong correlation with the measured trace metals, and the highest correlation is observed with Cu and Zn. Samira and El-Din (2001) assert that Cu and Zn are more easily absorbed by *Ammonia* than the other elements. Copper, usually found at high concentration in estuarine environmental, may impact the food source, habitat, and symbionts of foraminifers (Carnahan et al., 2008). *Ammonia tepida* is sensitive to a low concentration of Cu, although it survived under a high Cu concentration. The lowest copper concentration in seawater is 10 $\mu g\ l^{-1}$, and the lethal value is between 200 and 400 $\mu g\ l^{-1}$ (Le Cadre and Debenay, 2006). We found that *Ammonia tepida* is absent from the foraminiferal assemblage as the water depth increases to 30–40 m (Fig. 4a); meanwhile, the Cu concentration decreases to less than 20 $mg\ kg^{-1}$ in sediments (Fig. 2f). Some shallow-water species, including *Elphidium nakanokawaense Cavarotalia annectens*, *Arenoparella asiatica Ammoscalaria* sp., *Ammobaculites agglutinans*, *Cribrononion* sp., and *Haplophragmoides canariensis*, are characteristic in the most highly polluted area. These species might be moderately tolerant to pollution. Although X-ray microanalysis reveals that deformed living specimens contain higher concentrations of trace elements (Pb, Zn, Cu, Cr and Cd) than non-deformed specimens (Samira and El-Din, 2001), little is known about the physiological response of foraminifera to trace metal pollution (Le Cadre and Debenay, 2006; Martins et al., 2010; Samira and El-Din, 2001).

In the CCA analysis, the contents of Ba, Cu, Co, Cr, Ni, Pb, Sr, V, Zn, Zr, organic carbon, sand and clay were selected as environmental variables. A good positive correlation can be observed between the first axis and Cu and Pb, whereas a highly negative correlation can be observed between the second axis and Ba. The correlation between the two axes and the other variables is poor. Thus, Cu, Pb and Ba determine the distribution patterns of foraminifera. Other variables play a minor role in foraminiferal assemblages, although these variables contribute to the environmental influence of these assemblages.

The CCA results (Fig. 7) illustrate that the *A*1 axis is positively linked with Cu, Pb, Co, Cr, Ni, V, and Zn, and the *A*2 axis is positively linked with Ba. The sampling site groups are suggested to be separated on the two axes. The correlation matrix (Table 2) reveals that trace metals such as Cu, Pb, Co, Cr, Ni, V, and Zn have a positive effect on characteristic species of sampling site group B while a negative effect is observed for characteristic species of groups A, C, and D. Barium is negatively correlated with characteristic species of group D while positively correlated with characteristic species of group A.

Foraminifera can benefit from organic materials as a source of nutrients (Alve, 1995). Microorganisms utilize biodegradable substances as a source of carbon and energy, and foraminifera may feed on these bacteria (Murray, 2006). However, the excess flux of organic materials can cause algal blooms and the rapid consumption of oxygen, which ultimately lead to oxygen deficiency in the sediment–water interface (Pearson and Rosenberg, 1976). Oxygen is a critical factor for the survival of benthic foraminifera (Panchang et al., 2006). The foraminiferal community in an oxygen-deficient environment is characterized by an abundance of *Ammonia tepida* and other species (Donnici and Serandrei Barbero, 2002). In this study, we verify that *Ammonia tepida* is very numerous in areas enriched with organic carbon. Furthermore, organic carbon measured in the studied area is negatively correlated with foraminiferal richness (Table 2). This finding indicates that organic carbon is a limiting factor for species diversity.

## 6. Conclusions

The surface sediments collected from 246 stations outside the Pearl River Estuary predominantly yielded 52 species of benthic foraminifera. The majority of foraminiferal assemblages belong to *Ammonia tepida*, *Hanzawaia nipponica*, *Ammonia ketienziensis*, *Elphidium advenum*, *Ammonia compressiuscula*, *Florilus japonicus*, *Heterolepa dutemplei* and *Gavelinopsis prageri*. Four sampling site groups were established on the basis of factor loadings by R-mode factor analysis. The CCA was used to relate the foraminifera data to a set of measured environmental factors. Copper, Pb and Ba are the determining factors for the distribution patterns of foraminifera, whereas other variables, including Co, Cr, Ni, Sr, V, Zn, Zr, organic carbon, sand and clay, play a minor role in foraminiferal assemblages.

The spatial distributions of trace metals (Co, Cr, Cu, Ni, Pb, Zn) are controlled by the dispersion of sedimentary material. The sites that are most highly polluted with Cr, Cu, Pb and Zn with the lowest levels of $H(S)$, Fisher $\alpha$ index, and number of species are located in the western coastal zone. *Ammonia tepida* is the most abundant species in the most highly polluted area and is recognized as the only bioindicator of trace metal pollutants and organic carbon. This species has the strongest correlation with Cu and Zn. Organic carbon is a limiting factor for the foraminiferal community, and *Ammonia tepida* is abundant in sediment containing a large amount of organic matter.

## Acknowledgements

We would like to thank the crew on the marine survey cruise in the Pearl River Estuary for the sampling work. We also extend our thanks to anonymous reviewers for their constructive comments and suggestions, which have helped improve this paper. This work is supported by the National Natural Science Foundation of China (91228207).

## Appendix A. Supplementary material

Supplementary data associated with this article can be found, in the online version, at http://dx.doi.org/10.1016/j.marpolbul.2013.07.055.

## References

Alve, E., 1995. Benthic foraminiferal responses to estuarine pollution: a review. J. Foramin. Res. 25, 190–203.

Alve, E., Lepland, A., Magnusson, J., Backer-Owe, K., 2009. Monitoring strategies for re-establishment of ecological reference conditions: possibilities and limitations. Mar. Pollut. Bull. 59, 297–310.

Alve, E., Nagy, J., 1986. Estuarine foraminiferal distribution in Sandebukta, a branch of the Oslo fjord. J. Foramin. Res. 16, 261–283.

Alve, E., Olsgard, F., 1999. Benthic foraminiferal colonization in experiments with copper-contaminated sediments. J. Foramin. Res. 29, 186–195.

Armynot du Châtelet, E., Debenay, J.P., Soulard, R., 2004. Foraminiferal proxies for pollution monitoring in moderately polluted harbours. Environ. Pollut. 127, 27–40.

Armynot du Châtelet, E.A., Gebhardt, K., Langer, M.R., 2011. Coastal pollution monitoring: foraminifera as tracers of environmental perturbation in the port of Boulogne-sur-Mer (Northern France). N. Jb. Geol. Paläont. Abh. 262, 91–116.

Bergamin, L., Romano, E., Finoia, M.G., Venti, F., Bianchi, J., Colasanti, A., Ausili, A., 2009. Benthic foraminifera from the coastal zone of Baia (Naples, Italy): assemblage distribution and modification as tools for environmental characterisation. Mar. Pollut. Bull. 59, 234–244.

Bergamin, L., Romano, E., Gabellini, M., Ausili, A., Carboni, M.G., 2003. Chemical–physical and ecological characterisation in the environmental project of a polluted coastal area: the Bagnoli case study. Mediterranean Mar. Sci. 4, 5–20.

Bergamin, L., Romano, E., Magno, M.C., Ausili, A., Gabellini, M., 2005. Pollution monitoring of Bagnoli Bay (Tyrrhenian Sea, Naples, Italy), a sedimentological, chemical and ecological approach. Aquat. Ecosyst. Health Manage. 8, 293–302.

Bergin, F., Kucuksezgin, F., Uluturhan, E., Barut, I.F., Meric, E., Avsar, N., Nazik, A., 2006. The response of benthic foraminifera and ostracoda to heavy metal pollution in Gulf of Izmir (Eastern Aegean Sea). Estuar. Coast. Shelf Sci. 66, 368–386.

Blott, S.J., Pye, K., 2001. GRADISTAT: a grain size distribution and statistics package for the analysis of unconsolidated sediments. Earth Surf. Proc. Land. 26, 1237–1248.

Carnahan, E.A., Hoare, A.M., Hallock, P., Lidz, B.H., Reich, C.D., 2008. Distribution of heavy metals and Foraminiferal assemblages in sediments of Biscayne bay, Florida, USA. J. Coastal Res. 24, 159–169.

Chen, J.S., Zhou, J.Y., 1992. Heavy Metal Research in the Aquatic Environment of China. Environmental Science Press of China, Beijing, China, p. 387.

Clarke, K.R., Gorley, R.N., 2001. PRIMER v5: User Manual/Tutorial. PRIMER-E Ltd., Plymouth, p. 91.

Debenay, J.P., Fernandez, J.M., 2009. Benthic foraminifera records of complex anthropogenic environmental changes combined with geochemical data in a tropical bay of New Caledonia (SW Pacific). Mar. Pollut. Bull. 59, 311–322.

Debenay, J.P., Guillou, J.J., Redois, F., Geslin, E., 2000. Distribution trends of foraminiferal assemblages in paralic environments. In: Martin, R. (Ed.), Environmental Micropaleontology. Kluwer Academic/Plenum Publishers, New York, pp. 39–67.

Debenay, J.P., Tsakiridis, E., Soulard, R., Grossel, H., 2001. Factors determining the distribution of foraminiferal assemblages in Port Joinville Harbor (Ile d'Yeu, France): the influence of pollution. Mar. Micropaleontol. 43, 75–118.

Donnici, S., Serandrei Barbero, R., 2002. The benthic foraminiferal communities of the northern Adriatic continental shelf. Mar. Micropaleontol. 44, 93–123.

Du, J.Z., Mu, H.D., Song, H.Q., Yan, S.P., Gu, Y.J., Zhang, J., 2008. 100 years of sediment history of heavy metals in Daya Bay, China. Water Air Soil Pollut. 190, 343–351.

Eichler, P.P.B., Eichler, B.B., Gupta, B.S., Rodrigues, A.R., 2012. Foraminifera as indicators of marine pollutant contamination on the inner continental shelf of southern Brazil. Mar. Pollut. Bull. 64, 22–30.

Elberling, B., Knudsen, K.L., Kristensen, P.H., Asmund, G., 2003. Applying foraminiferal stratigraphy as a biomarker for heavy metal contamination and mining impact in a fiord in west Greenland. Mar. Environ. Res. 55, 235–256.

Ferraroa, L., Sprovieria, M., Albericob, I., Lirera, F., Prevedelloa, L., Marsellaa, E., 2006. Benthic foraminifera and heavy metals distribution: a case study from the Naples Harbour (Tyrrhenian Sea, Southern Italy). Environ. Pollut. 142, 274–287.

Fisher, R.A., Corbet, A.S., Williams, C.B., 1943. The relationship between the number of species and the number of individuals in a random sample of an animal population. J. Anim. Ecol. 12, 42–58.

Foster, W.J., Châtelet, E.A.d., Rogerson, M., 2012. Testing benthic foraminiferal distributions as a contemporary quantitative approach to biomonitoring estuarine heavy metal pollution. Mar. Pollut. Bull. 64, 1039–1048.

Frontalini, F., Buosi, C., Da Pelo, S., Coccioni, R., Cherchi, A., Bucci, C., 2009. Benthic foraminifera as bio-indicators of trace element pollution in the heavily contaminated Santa Gilla lagoon (Cagliari, Italy). Mar. Pollut. Bull. 58, 858–877.

Frontalini, F., Coccioni, R., 2008. Benthic foraminifera for heavy metal pollution monitoring: A case study from the central Adriatic Sea coast of Italy. Estuar. Coast. Shelf Sci. 76, 404–417.

Frontalini, F., Coccioni, R., 2011. Benthic foraminifera as bioindicators of pollution: a review of Italian research over the last three decades. Rev. Micropaléontol. 54, 115–127.

Gao, S., 1996. A Fortran program for grain-size trend analysis to define sand sediment transport pathways. Comput. Geosci. 22, 449–452.

Gao, S., Collins, M., 1991. A critique of the McLaren method for defining sediment transport paths: discussion. J. Sediment. Petrol. 61, 143–146.

Gao, S., Collins, M., 1992. Sand sediment transport patterns inferred from grain-size trends based upon definition of "transport vectors". Sed. Geol. 80, 47–60.

Gao, S., Collins, M., 1994a. Analysis of grain size trends, for defining sediment transport pathways in marine environments. J. Coastal Res. 10, 70–78.

Gao, S., Collins, M., 1994b. Net sediment transport patterns inferred from grain-size trends, based upon definition of "transport vectors"—reply. Sed. Geol. 90, 157–159.

Ip, C., Li, X., Zhang, G., Farmer, J.G., Wai, W.O., Li, Y., 2004. Over one hundred years of trace metal fluxes in the sediments of the Pearl River Estuary, South China. Environ. Pollut. 132, 157–172.

Le Cadre, V., Debenay, J.-P., 2006. Morphological and cytological responses of Ammonia (foraminifera) to copper contamination: implication for the use of foraminifera as bioindicators of pollution. Environ. Pollut. 143, 304–317.
Li, T., Xiang, R., Li, T., 2011. Benthic foraminiferal assemblages in surface sediments off the Pearl River Estuary and their environmental implications. J. Tropical Oceanography 30, 51–57 (in Chinese).
Li, X., 2003. Distribution of heavy metals in substrate of the Daya Bay, Guangdong, and assessment of the quality of the seafloor environment. Geol. China 30, 429–435 (in Chinese).
Li, X., Shen, Z., Wai, O.W.H., Li, Y.-S., 2000. Chemical partitioning of heavy metal contaminants in sediments of the Pearl River Estuary. Chem. Speciat. Bioavailab. 12, 17–25.
Ligero, R.A., Barbera, M., Casas-Ruiz, M., Sales, D., Lopez-Aguayo, F., 2002. Dating of marine sediments and time evolution of heavy metal concentration in the Bay of Cadiz, Spain. Environ. Pollut. 118, 97–108.
Long, E.R., MacDonald, D.D., Smith, S.L., Calder, F.D., 1995. Incidence of adverse biological effects within ranges of chemical concentrations in marine and estuarine sediments. Environ. Manage. 19, 81–97.
Martins, V., Silva, E.F.d., Sequeira, C., Rocha, F., Duarte, A.C., 2010. Evaluation of the ecological effects of heavy metals on the assemblages of benthic foraminifera of the canals of Aveiro (Portugal). Estuar. Coast. Shelf Sci. 87, 293–304.
Martins, V.A., Frontalini, F., Tramonte, K.M., Figueira, R.C.L., Miranda, P., Sequeira, C., Fernández-Fernández, S., Dias, J.A., Yamashita, C., Renó, R., Laut, L.L.M., Silva, F.S., Rodrigues, M.A.d.C., Bernardes, C., Nagai, R., Sousa, S.H.M., Mahiques, M., Rubio, B., Bernabeu, A., Rey, D., Rocha, F., 2013. Assessment of the health quality of Ria de Aveiro (Portugal): Heavy metals and benthic foraminifera. Marine Pollution Bulletin. <http://dx.doi.org/10.1016/j.marpolbul.2013.02.003>.
Milligan, T.G., Loring, D.H., 1997. The effect of flocculation on the size distributions of bottom sediment in coastal inlets: implications for contaminant transport. Water Air Soil Pollut. 99, 33–42.
Murray, J.W., 2000. When does environmental variability become environmental change? The Proxy Record of benthic Formanifera. In: Martin, R.E. (Ed.), Environmental Micropaleontology. Plenum Publishing Co., New York, pp. 3–37.
Murray, J.W., 2006. Ecology and applications of benthic foraminifera. Cambridge University Press, New York, p. 440.
Ongley, E.D., Krishnappan, B.G., Droppo, G., Rao, S.S., Maguire, R.J., 1992. Cohesive sediment transport: emerging issues for toxic chemical management. Hydrobiologia 235–236, 177–187.
Panchang, R., Nigam, R., Linshy, V., Rana, S., Ingole, B., 2006. Effect of oxygen manipulations on benthic foraminifera: a preliminary experiment. Indian J. Mar. Sci. 35, 235–239.
Pati, P., Patra, P.K., 2012. Benthic foraminiferal responses to coastal pollution: a review. Int. J. Geol., Earth Environ. Sci. 2, 42–56.
Pearson, T.H., Rosenberg, R., 1976. Macrobenthos succession in relatin to organic enrichment and pollution of the marine environment: oceanography and Marine Biology. Ann. Rev. 16, 229–311.
Qiu, Y., Yan, W., Wang, Z., Zhang, G., 2005. Distributions of heavy metals in seawater, sediments and organisms at Daya Bay and their ecological harm. J. Tropical Oceanography 24, 69–76 (in Chinese).
Romano, E., Bergamin, L., Ausili, A., Pierfranceschi, G., Maggi, C., Sesta, G., Gabellini, M., 2009. The impact of the Bagnoli industrial site (Naples, Italy) on sea-bottom environment. Chemical and textural features of sediments and the related response of benthic foraminifera. Mar. Pollut. Bull. 59, 245–256.
Romano, E., Bergamin, L., Finoia, M.G., Carboni, M.G., Ausili, A., Gabellini, M., 2008. Industrial pollution at Bagnoli (Naples, Italy): benthic foraminifera as tool in integrated programs of environmental monitoring. Mar. Pollut. Bull. 56, 439–457.
Samir, A.M., 2000. The response of benthic foraminifera and ostracods to various pollution sources: a study from two lagoons in Egypt. J. Foramin. Res. 30, 83–98.
Samira, A.M., El-Din, A.B., 2001. Benthic foraminiferal assemblages and morphological abnormalities as pollution proxies in two Egyptian bays. Mar. Micropaleontol. 41, 193–227.
Sánchez, A., Carriquiry, J.D., 2011. Sediment transport patterns in Todos Santos Bay, Baja California, Mexico, inferred from grain-size trends. In: Manning, A.J. (Ed.), Sediment Transport in Aquatic Environments. InTech, pp. 1–18.
Schafer, C.T., 1973. Distribution of foraminifera near pollution sources in Chaleur Bay. Water Air Soil Pollut. 2, 219–233.
Shannon, C.E., 1948. A mathematical theory of communication. Bell Syst. Tech. J. 27, 379–423.
Shepard, F.P., 1954. Nomenclature based on sand, silt, clay ratios. J. Sediment. Petrol. 24, 151–158.
Su, J., 2004. Overview of the South China Sea circulation and its influence on the coastal physical oceanography outside the Pearl River Estuary. Cont. Shelf Res. 24, 1745–1760.
Szarek, R., Kuhnt, W., Kawamura, H., Kitazato, H., 2006. Distribution of recent benthic foraminifera on the Sunda Shelf (South China Sea). Mar. Micropaleontol. 61, 171–195.
Teodoro, A.C., Duleba, W., Gubitoso, S., Prada, S.M., Lamparelli, C.C., Bevilacqua, J.E., 2010. Analysis of foraminifera assemblages and sediment geochemical properties to characterise the environment near Araçá and Saco da Capela domestic sewage submarine outfalls of São Sebastião Channel, São Paulo State, Brazil. Mar. Pollut. Bull. 60, 536–553.
Wong, C., Chu, K., Chen, Q., Ma, X., 1995. Environmental Research in Pearl River and Coastal Areas. Guangdong Higher Education Press, Guangzhou, China, p. 192. (in Chinese).
Wong, L.A., Chen, J.C., Xue, H., Dong, L.X., Su, J.L., Heinke, G., 2003. A model study of the circulation in the Pearl River Estuary (PRE) and its adjacent coastal waters: 1. Simulations and comparison with observations. Journal of Geophysical Research. Oceans (1978–2012) 108, 3156, doi: 3110.1029/2002JC001451.
Yanko, V., Ahmad, M., Kaminsky, M., 1998. Morphological deformities of benthic foraminiferal tests in response to pollution by heavy metals: implications for pollution monitoring. J. Foramin. Res. 28, 177–200.
Yin, K., Qian, P.-Y., Chen, J.C., Harrison, P.J., 2000. Dynamics of nutrients and phytoplankton biomass in the Pearl River Estuary and adjacent waters of Hong Kong during summer: preliminary evidence for phosphorus and silicon limitation. Mar. Ecol. Prog. Ser. 194, 295–305.
Yu, X., Yan, Y., Wang, W.-X., 2010. The distribution and speciation of trace metals in surface sediments from the Pearl River Estuary and the Daya Bay, Southern China. Mar. Pollut. Bull. 60, 1364–1371.
Zheng, Q., Liang, Z., He, Y., Wen, W., 1992. Geochemical behaviour of the pollutants in surface sediments of Daya Bay. Tropic Oceanol. 11, 65–71 (in Chinese).